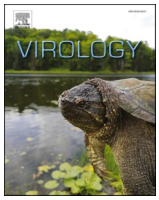
Virology 596 (2024) 110125



Contents lists available at ScienceDirect

Virology

journal homepage: www.elsevier.com/locate/virology





A combination influenza mRNA vaccine candidate provided broad protection against diverse influenza virus challenge

Yuying Tian [a,c], Zhuoya Deng [a], Zhengran Chuai [b], Cong Li [a,c], Liangzheng Chang [a], Fang sun [b], Rui Cao [a,c], Hongyu Yu [a,c], Ruixue Xiao [a,c], Shuai Lu [a], Yan Xu [a], Penghui Yang [a,c,*]

[a] Faculty of Hepato-Pancreato-Biliary Surgery, Institute of Hepatobiliary Surgery, The First Medical Center, Chinese PLA General Hospital, Beijing, 100853, China
[b] The Fifth Medical Center, Chinese PLA General Hospital, Beijing, 100039, China
[c] School of Basic Medicine, Inner Mongolia Medical University, Hohhot, China

ARTICLE INFO

Handling Editor: Jasmine Tomar

Keywords:
mRNA vaccine
Influenza viruses
Influenza viruses mRNA vaccine
Immunoprotection

ABSTRACT

Influenza viruses present a significant threat to global health. The production of a universal vaccine is considered essential due to the ineffectiveness of current seasonal influenza vaccines against mutant strains. mRNA technology offers new prospects in vaccinology, with various candidates for different infectious diseases currently in development and testing phases. In this study, we encapsulated a universal influenza mRNA vaccine. The vaccine encoded influenza hemagglutinin (HA), nucleoprotein (NP), and three tandem repeats of matrix protein 2 (3M2e). Twice-vaccinated mice exhibited strong humoral and cell-mediated immune responses in vivo. Notably, these immune responses led to a significant reduction in viral load of the lungs in challenged mice, and also conferred protection against future wild-type H1N1, H3N2, or H5N1 influenza virus challenges. Our findings suggest that this mRNA-universal vaccine strategy for influenza virus may be instrumental in mitigating the impact of future influenza pandemics.

1. Introduction

Over the last century, flu pandemics have had devastating impacts on human populations, resulting in millions of deaths and hundreds of millions of illnesses. The Centers for Disease Control and Prevention (CDC) reported that between October 1, 2022, and March 18, 2023, there were 26–52 million flu cases and 18,000–56,000 flu-related deaths (CDC). The World Health Organization (WHO), through the Global Influenza Detection and Response System, collaborates with various international organizations to provide semi-annual guidance on seasonal influenza vaccine formulations for both the northern and southern hemispheres. According to the U.S. CDC, flu vaccine effectiveness ranged from 10% to 60% between 2004 and 2019 (Cdc Seasonal Flu Vaccine Effectiveness). The current seasonal influenza vaccines aim to induce a specific neutralizing antibody response to the influenza hemagglutinin (HA) heads (Krammer, 2019). However, due to antigenic drift, which is a continuous process of viral evolution, the HA head domain is prone to mutations (Heaton et al., 2013). Consequently, vaccines may not be effective against new influenza subtypes, failing to offer lifelong protection (Kim et al., 2018). Most approved vaccines are egg-based, which can lead to virus adaptation and reduced vaccine efficacy (Zost et al., 2017). Additionally, the antibody response is often temporary in many vaccine recipients, with antibody levels dropping to sub-protective levels before the end of the flu season (Ainslie et al., 2019). The good safety profile of mRNA vaccines, their high immunogenicity in the context of humoral and cellular immune responses, ability to design the sequences to encode optimized version of antigen, and rapid manufacturing pace, provide novel opportunities for influenza prevention (Rzymski et al., 2023).

The concept of mRNA vaccination involves delivering mRNA that encodes one or more antigen proteins to host cells, which then directly translate these proteins in the cytoplasm, triggering specific immune responses in the body (Ozdilek et al., 2020). The idea of introducing mRNA to prompt cells to produce a specific protein dates to 1976–1978. In the early 1990s, the potential for mRNA use in vaccination was suggested (Martinon et al., 1993), but it faced several challenges including the instability of the mRNA molecule, its recognition by Toll-like receptors (Tan et al., 2020), and delivery issues (Leppek et al., 2022). In

* Corresponding author. Faculty of Hepato-Pancreato-Biliary Surgery, Institute of Hepatobiliary Surgery, The First Medical Center, Chinese PLA General Hospital, Beijing, 100853, China.
E-mail address: ypenghuiamms@hotmail.com (P. Yang).

https://doi.org/10.1016/j.virol.2024.110125
Received 29 August 2023; Received in revised form 19 May 2024; Accepted 23 May 2024
Available online 23 May 2024
0042-6822/© 2024 Elsevier Inc. This article is made available under the Elsevier license (http://www.elsevier.com/open-access/userlicense/1.0/).

the past ten years, the above issues have been gradually solved. These problems were addressed through nucleoside modification (Karikó et al., 2005; Andries et al., 2015) and the development of lipid nanoparticles (LNPs) as vehicles (Hald et al., 2022) for mRNA molecules. The advantages of mRNA vaccines include rapid development, flexibility, non-infectious nature, robust immunity, simplified manufacturing, rapid modification capabilities, safety, and versatility (Kim et al., 2021; Dolgin, 2021).There are other mRNA projects against influenza, including tetravalent influenza vaccines (NCT06020118), combined COVID-19 and influenza vaccines (NCT05650554), and universal vaccines that are currently in clinical trials (NCT05755620, NCT06028347). And there is a vaccine encoding 20 HAs to protected mice from viral challenge (Arevalo et al., 2022).

To establish an experimental and theoretical basis for designing mRNA candidate influenza vaccines and developing immunization strategies, we developed influenza mRNA vaccines expressing influenza virus HA, nucleoprotein (NP), and the extracellular region of matrix proteins. We conducted immunization experiments and protective evaluation challenges for these vaccines using the Balb/c mice animal model.

2. Materials and methods

2.1. Viruses and cells

The influenza A viruses used in this study included H1N1 (A/Beijing/501/2009), H3N2 (A/Wisconsin/67/2005), and H5N1 (A/Ostrich/SuZhou/097/2003). All viruses were cultured in 9-day-old specific pathogen-free (SPF) chicken embryos (Beijing Boehringer Ingelheim Viton Biotechnology Co., Ltd., Beijing, China), incubated at 33 °C for 72 h and then at 4 °C overnight. The allantoic fluid was extracted from each embryo through centrifugation at 4000 rpm for 40 min to separate debris. The fluid was then purified using sucrose and stored at −80 °C.

The cell lines used in this study included HEK293T, Madin–Darby Canine Kidney (MDCK), A549, and HeLa cells, all sourced from the American Type Culture Collection (Manassas, VA, USA). These cell lines were cultured in Dulbecco's Modified Eagle's Medium (DMEM, Biosharp, Beijing, China), supplemented with 10% fetal bovine serum (FBS, Gibco) and 1% penicillin/streptomycin (Gibco).

QIV is quadrivalent split influenza virus vaccine. It contains hemagglutinin of prevalent strains of influenza virus: A/Victoria/2570/2019 (H1N1) pdm09-like virus, A/Darwin/9/2021(H3N2)-like virus, B/Austria/1359417/2021(B/Victoria lineage)-like virus, B/Phuket/3073/2013(B/Yamagata lineage)-like virus.

2.2. mRNA preparation

We analyzed strain A/California/04/2009 alongside WHO-recommended vaccine strains from the past two years and prevalent influenza A strains in China (Table 1 and 2). We selected the full-length HA fragment to ensure strong immune response; NP and M2e proteins are highly conserved, and we linked three M2e sequences (3M2e) to enhance the immune response.

We designed the HA, NP, and three tandem M2e repeat (3M2e) sequences of the A/California/04/2009 strain within the pcDNA3.1 vector

Table 1
Nucleotide sequence homology between modified vaccine antigens and corresponding influenza virus proteins.

	Name	HA %	NP %	M2e %
H1N1	A/Beijing/501/2009	94.21	99.87	100.00
H1N1	A/Victoria/2570/2019	95.72	97.47	97.60
H1N1	A/Victoria/4897/2022	94.65	–	97.56
H3N2	A/Darwin/9/2021	46.93	81.96	85.73
H3N2	A/Wisconsin/67/2005	46.98	82.95	90.00
H5N1	A/Ostrich/Suzhou/097/2003	64.60	83.45	97.14

Table 2
Amino acid sequence homology between modified vaccine antigens and corresponding influenza virus proteins.

		HA %	NP %	M2e %
H1N1	A/Beijing/501/2009	99.47	99.80	100.00
H1N1	A/Victoria/2570/2019	94.88	99.00	92.31
H1N1	A/Victoria/4897/2022	93.11	–	92.31
H3N2	A/Darwin/9/2021	42.37	89.16	80.77
H3N2	A/Wisconsin/67/2005	42.19	90.56	97.14
H5N1	A/Ostrich/Suzhou/097/2003	63.30	93.78	100.00

Improved nucleotide and amino acid sequence homology between vaccine antigens and corresponding influenza virus proteins using DNAMAN multiple sequence alignment.

(Sangon Biotech, Shanghai, China). The plasmids were linearized using the restriction endonuclease EcoR1(NEB #R3101) and purified (NEB #T1030) as templates for in vitro transcription. For the synthesis of modified nucleoside-containing mRNA, the DNA template was transcribed in vitro using N1–Me-Pseudo UTP (Vazyme DD4202). A 7-methylguanoside Cap structure (m7Gppp, Cap0) was added to the 5′-end of the RNA, and the mRNA Cap 2′-*O*-methyltransferase transferred a methyl group from the donor molecule SAM to the 2′-O position of the first nucleotide adjacent to the cap. This process transformed Cap 0-RNA into Cap 1-RNA (Novoprotein, GMP-M072-M062). A poly(A) tail was added at the end of the 3′UTR (Novoprotein, GMP-M012). High-purity mRNA was obtained using RNA Clean Beads (Vazyme N412).

To prepare LNPs, liposome components were dissolved in ethanol as the organic phase in the ratio of 50:10:38.5:1.5 (DLin-MC3-DMA:DSPC:cholesterol:DSPE-PEG2000). The mRNA was dissolved in a 50 mM acetate buffer (pH 4.3) as the aqueous phase at a concentration of 200 μg/mL. The organic and aqueous phases were combined through a microfluidic chip in a 1:3 flow volume ratio to produce LNP-mRNA.

In the initial assay, a gradient-diluted standard (20 μg), 10 μL of LNP-mRNA plus 10 μL of 5% Triton X-100, and 10 μL of LNP plus 10 μL of PBS were mixed with RiboGreen dye as recommended. This mixture was incubated for 5 min to allow the formation of fluorescent complexes via the binding of the dye to nucleic acids. The fluorescence intensity of the samples was then measured using a fluorescence spectrophotometer. Encapsulation efficiency was calculated using the formula: Encapsulation efficiency (%) = (1 − Total mRNA concentration/Unencapsulated mRNA concentration) × 100%.

Dynamic light scattering (DLS) and zeta potential measurements of the mRNA-LNP were performed using a Zeta sizer Nano instrument (Malvern, UK) at 25 °C. Before the measurements, samples were diluted 1000-fold with PBS. Each sample underwent at least three measurements, with results expressed as intensity-weighted size distributions.

2.3. Western blot

The 293T, MDCK, A549, and HeLa cells were seeded in 6-well plates and transfected with Lipofectamine 3000 (Invitrogen) at 80% confluence, using 2.5 μg of mRNA per well. Cells were collected and lysed with RIPA buffer (Huaxingbio, HX1862). The HA and NP proteins underwent electrophoresis using 10% sodium dodecyl sulfate polyacrylamide gel electrophoresis (SDS-PAGE), and 3M2e was processed with 15% SDS-PAGE, followed by Western blotting. The proteins were detected using specific antibodies: anti-HA mouse monoclonal antibody for HA protein (1:500 dilution, GeneTex, GTX28262), anti-NP rabbit polyclonal antibody for NP protein (1:3000 dilution, GeneTex, GTX636247), and anti-M2 rabbit monoclonal antibody for the 3M2e protein (1:3000 dilution, GeneTex, GTX125951). Detection was followed by the application of HRP-conjugated secondary goat anti-rabbit (1:10,000 dilution, ZSGB-bio, ZB2306) and goat anti-mouse antibodies (1:10,000 dilution, Protentech, Cat No. SA00001-1), respectively.

2.4. Immunofluorescence

Immunofluorescence analysis was conducted to assess the expression of HA-mRNA, NP-mRNA, and 3M2e-mRNA in 293T, MDCK, A549, and HeLa cells. Cells were seeded in 24-well plates on 14-mm glass slides (NEST 801010) at a density of 1 × 105 cells per well and transfected the following day using Lipofectamine 3000. After 24 h, cells were fixed i with 4% paraformaldehyde, permeabilized using 0.5% Triton X-100 in PBS, and then incubated in a 5% BSA blocking solution for 30 min. Overnight incubation with primary antibodies for HA, NP, and M2 (GeneTex, GTX28262, GTX636247, GTX125951) was followed by three washes in PBST. Secondary antibodies, including Alexa Fluor 488-labelled goat anti-rabbit IgG H&L (1:500, Abcam ab150077) and Alexa Fluor 350-labelled goat anti-mouse IgG H&L (1:500, Beyotime A0412), were then incubated at room temperature in the dark for 1 h. After three PBS washes, the glass slides were carefully extracted using forceps and mounted on slides with DAPI (Huaxingbio, HXJ3109) sealer. Photographs Imaging was performed using an orthomorphic fluorescence microscope.

2.5. Immunization of mice and virus challenge

Female Balb/c mice, aged 6–8 weeks, were immunized intramuscularly with 50 μL of the mRNA vaccine (4.5 μg) in the left thigh. A commercial split, quadrivalent influenza-vaccinated (QIV) as control. Four weeks later, a similar dose was administered in the right thigh. Two weeks after the booster, mice were anesthetized and intranasally infected with 30 μL of $5LD_{50}$ influenza virus. Weight loss was monitored for 14 days; mice losing more than 25% of their initial body weight were humanely euthanized. Blood samples were taken on days −1, 27, and 42 after vaccination for serological analysis. All procedures involving mice were approved by the Animal Welfare and Ethics Committee of the First Medical Centre of the Chinese People's Liberation Army General Hospital.

2.6. Hemagglutinin inhibition (HI) assay

HI testing was performed using virus stock solutions of A/Beijing/501/2009 (H1N1), A/Wisconsin/67/2005 (H3N2), and A/Ostrich/Suzhou/097/2003 (H5N1). Sera were initially treated with a receptor-disrupting enzyme (RDE) in a 3:1 ratio and incubated overnight at 37 °C. The following day, they were heated in a 56 °C water bath for 30 min and subsequently 2 folds dilutions with PBS. HI assays were conducted in V-bottom 96-well plates using four viral hemagglutinating units (HAU) and 0.5% chicken red blood cells. For each strain, reference serum was used as a positive control on each assay plate. Additionally, each plate included a back-titration for determining the antigen dose (4 HAU/25 μL) and a negative control (PBS or original control serum). HI titers were defined as the highest serum dilution that completely inhibited hemagglutination. Valid results were considered only for plates with correct back-titration results and a reference serum titer within two times the expected value.

2.7. Microneutralization assay

MDCK cells were seeded in 96-well culture dishes at a density of 2.5 × 10^4 cells per well and incubated overnight at 37 °C in a 5% CO2 atmosphere. Serum samples were diluted in a 37 °C water bath using RDE (Seiken) at a 3:1 working ratio. The following day, RDE-treated sera were incubated at 56 °C for 30 min. To achieve a final 1:10 dilution, PBS was added at a 3:7 ratio. Sera were then serially diluted 1:2 in 96-well plates. Influenza viruses H1N1, H3N2, and H5N1 were prepared to 100 $TCID_{50}$ in complete medium, mixed with the RDE-treated serum, and incubated at 37 °C for 1 h. Concurrently, MDCK cells were rinsed with PBS. Then, 100 μL of the serum/virus mixture was added to each well and incubated at 33 °C for 72 h. The cell supernatant was then mixed with 0.5% chicken erythrocytes (Lampire Biological Laboratories, Pipersville, PA, USA) for analysis.

2.8. Flow cytometry

To analyze the T cell immune response in mice 7 days after booster immunization, spleens were harvested, and single cell suspensions were prepared in complete RPMI-1640 medium. Cells were pre-activated with Cell Activation Cocktail (423303, BioLegend San Diego, CA, USA) and HA , NP , 3M2e protein for 4–6 h. Staining was performed with BV510 anti-mouse CD3 (100234, BioLegend), fluorescein isothiocyanate (FITC) anti-mouse CD4 (100406, BioLegend), and PerCp-CY5-A anti-mouse CD8 (100734, BioLegend) for surface markers. For intracellular cytokines, cells were stained with PE anti-mouse IFN-γ (505808, BioLegend), BV421 anti-mouse IL-2 (503826, BioLegend), and PEcy7 anti-mouse IL-4 (504118, BioLegend) for 20 min at room temperature. Following staining, all cells were washed with permeabilization buffer and fixed at 4 °C until analysis. Data acquisition and visualization were conducted using FlowJo software.

2.9. Lung virus titers

Lungs were harvested from mice 4 days post-infection. Following harvest, lungs were homogenized in DMEM. Homogenates were clarified twice by centrifugation, collected supernatant and stored at −80 °C. Clarified lung homogenate samples were serially diluted 10-fold in the 96-well cell culture plates included MDCK cells with a monolayer density of 90%, and each sample was tested in quadruplicate. Plates were incubated for 3 days in a 37 °C humidified incubator supplemented with 5% CO2. The results were interpreted by measuring the hemagglutination titer of the cell supernatant.

2.10. Statistical analyses

Statistical analyses were conducted using Prism 9.0 software (GraphPad, San Diego, CA, USA). Data in Fig. 3 were analyzed using a two-tailed unpaired *t*-test (McMahon et al., 2022). Data comparisons in Figs. 2 and 4 were conducted using two-way analysis of variance (ANOVA) with Dunnett's correction for multiple comparisons. Significance was evaluated at $P < 0.05$ or adjusted $P < 0.05$ and a 95% confidence interval.

3. Results

3.1. Selection, expression, and identification of mRNA influenza A vaccine antigens

Influenza viruses are categorized into 18 subtypes based on their HA antigens, with the annual pandemic primarily caused by the H1N1 and H3N2 strains. Highly pathogenic avian influenza viruses, such as H5N1 and H7N9, also pose a significant threat to human health (Yip et al., 2020). We analyzed strain A/California/04/2009 alongside WHO-recommended vaccine strains from the past two years and prevalent influenza A strains in China (Table 1). We observed high variability in the HA segment across different isoforms, with mutations predominantly in the head region, whereas the stem remained relatively conserved. (Deng et al., 2018). Noting that HA stems elicit a limited immune response, we selected the full-length HA fragment as a vaccine antigen. To broaden the vaccine's spectrum, NP and M2e proteins, which are highly conserved and induce strong immune responses, were also chosen as antigens. Given the short length of the M2e protein (26 amino acids), we linked three M2e sequences (3M2e) to enhance the immune response (Fig. 1a). Because A/California/04/2009 is the primary prevalent strain globally (Center and CNI, 2023), its HA, NP, and 3M2e sequences were selected as the antigen sequence for the mRNA influenza vaccine.

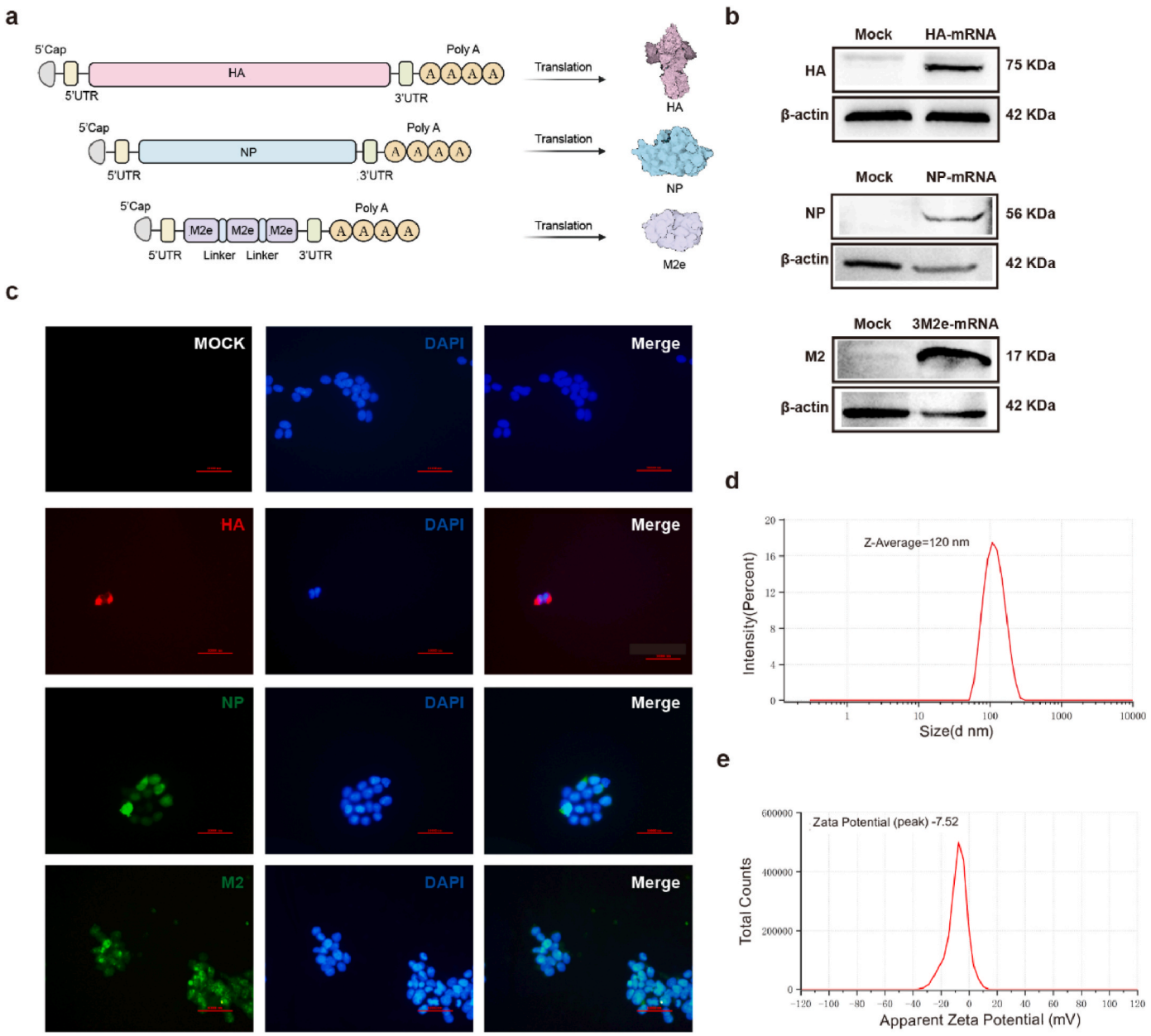


Fig. 1. Construction, expression and preparation of hemagglutinin (HA)-mRNA, nucleoprotein (NP)-mRNA, and triple-tandem matrix protein 2 (3M2e)-mRNA. (a) HA-mRNA, NP-mRNA, and 3M2e-mRNA sequence construction diagram. (b) Western blot and (c) immunofluorescence analyses verifying expression of HA-mRNA, NP-mRNA, and 3M2e-mRNA in transfected 293T cells after 24 h. (d) Particle size and (e) potential analysis of HA-mRNA, NP-mRNA, and 3M2e-mRNA encapsulated in lipid nanoparticles (LNPs).

We constructed the HA, NP, and 3M2e sequences of A/California/04/2009 in the pcDNA3.1 vector, linearizing the plasmid with a restriction endonuclease for in vitro transcription. The mRNA encoding HA, NP, and 3M2e sequences was synthesized using modified nucleotides, complete with cap and tail structures. This mRNA was transfected into 293T cells and confirmed through Western blotting (Fig. 1b) and immunofluorescence (Fig. 1c). Additionally, transfections into MDCK, Hela, and A549 cells were verified using Western blotting (Supplementary Fig. 1a-c) and immunofluorescence (Supplementary Fig. 2a-c) . LNPs were synthesized with a specific ratio of cationic lipids and other components to encapsulate HA-mRNA, NP-mRNA, and 3M2e-mRNA. These mRNAs exhibited particle sizes of 110–120 nm and a potential of −4 to −8 mV (Fig. 1d-e, Supplementary Figs. 3a–b), demonstrating high, stable encapsulation efficiency and good delivery potential.

3.2. Influenza mRNA vaccine effectively protects mice from H1N1 challenge

To assess the humoral immune response elicited by the mRNA vaccine, BALB/c mice were immunized with HA-mRNA, NP-mRNA, 3M2e-mRNA, and Comb-mRNA (a combination of the three vaccines) at a dosage of 4.5 μg mRNA per mouse. A booster was administered 28 days after the initial vaccination. A control group received equivalent doses of LNP (Fig. 2a). HI against strain A/Beijing/501/2009 (H1N1) indicated effective functional antibodies. After initial immunization, HA-mRNA exhibited HI titers of 80, and 142.5 after the booster; NP-mRNA and 3M2e-mRNA groups showed no HI titers; and Comb-mRNA presented HI titers of 89.8 for initial and 179.6 for booster vaccinations (Fig. 2b). The HA-mRNA group developed antibodies with HI titers significantly higher than those of the LNP group but lower than those of

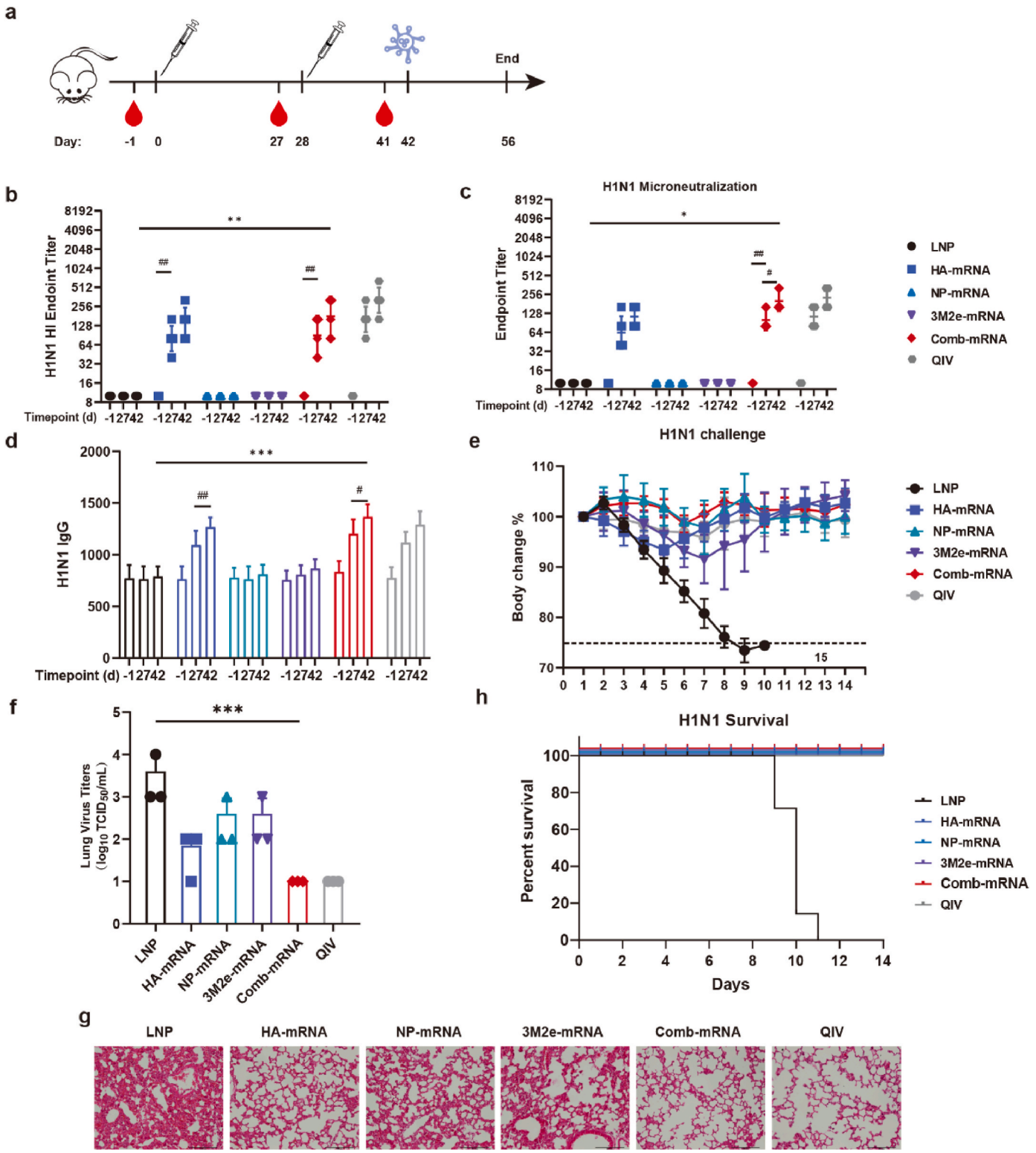


Fig. 2. Robust immune response in mice elicited by an mRNA vaccine encoding an influenza antigen. (a) Mice were inoculated twice with the LNP, HA-mRNA, NP-mRNA, 3M2e-mRNA, Comb-mRNA and 2021–2022 quadrivalent influenza virus vaccine (QIV) (4.5 μg per mouse per dose) at a 28-day interval. Blood samples were collected on days −1, 27, and 41, with a challenge on day 42. Analysis included six mice per group. (b) Hemagglutinin inhibition (HI) and (c) micro-neutralization titers for different mRNA vaccines evaluated at −1, 27, and 41 days after vaccination. Each point represents an individual animal. Line indicates the geometric mean of the group. Data are shown as geometrical mean ± 95% confidence intervals (CIs), analyzed by two-way ANOVA with multiple comparisons. (d) Serum total IgG levels detected using an enzyme-linked immunosorbent assay (ELISA). Data are expressed shown as means ± 95% CIs, analyzed by two-way analysis of variance (ANOVA). (e) Weight changes in mice after challenge with 5LD50 H1N1 influenza virus at 14 days following booster immunization. (n = 6) (h) Kaplan–Meier survival analysis after challenge with 5LD50 H1N1 influenza virus. (g) Pulmonary lesions and (f) viral load in mice 4 days after H1N1 virus challenge. Data are shown as means ± 95% CIs, analyzed by two-way ANOVA with multiple comparisons.

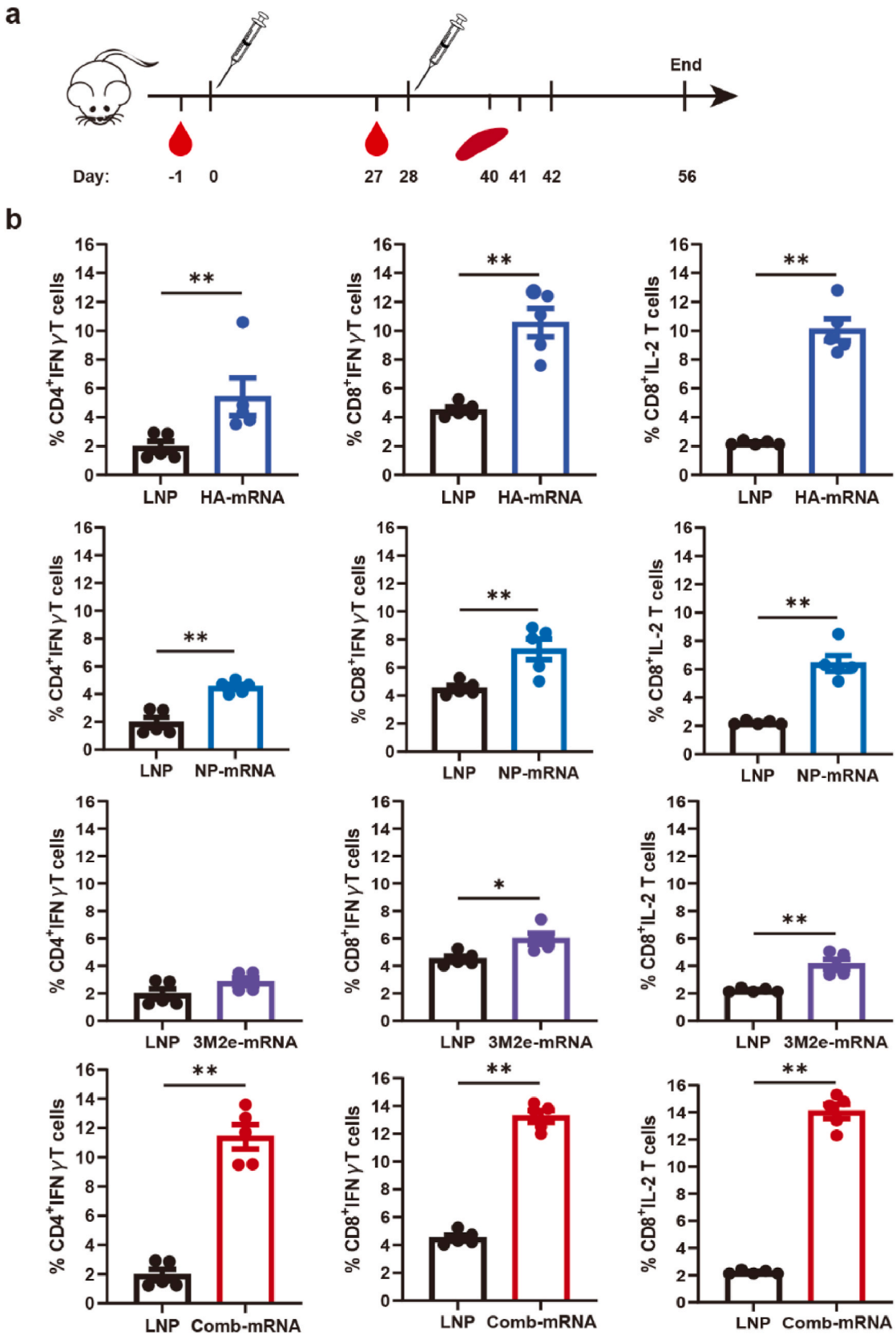
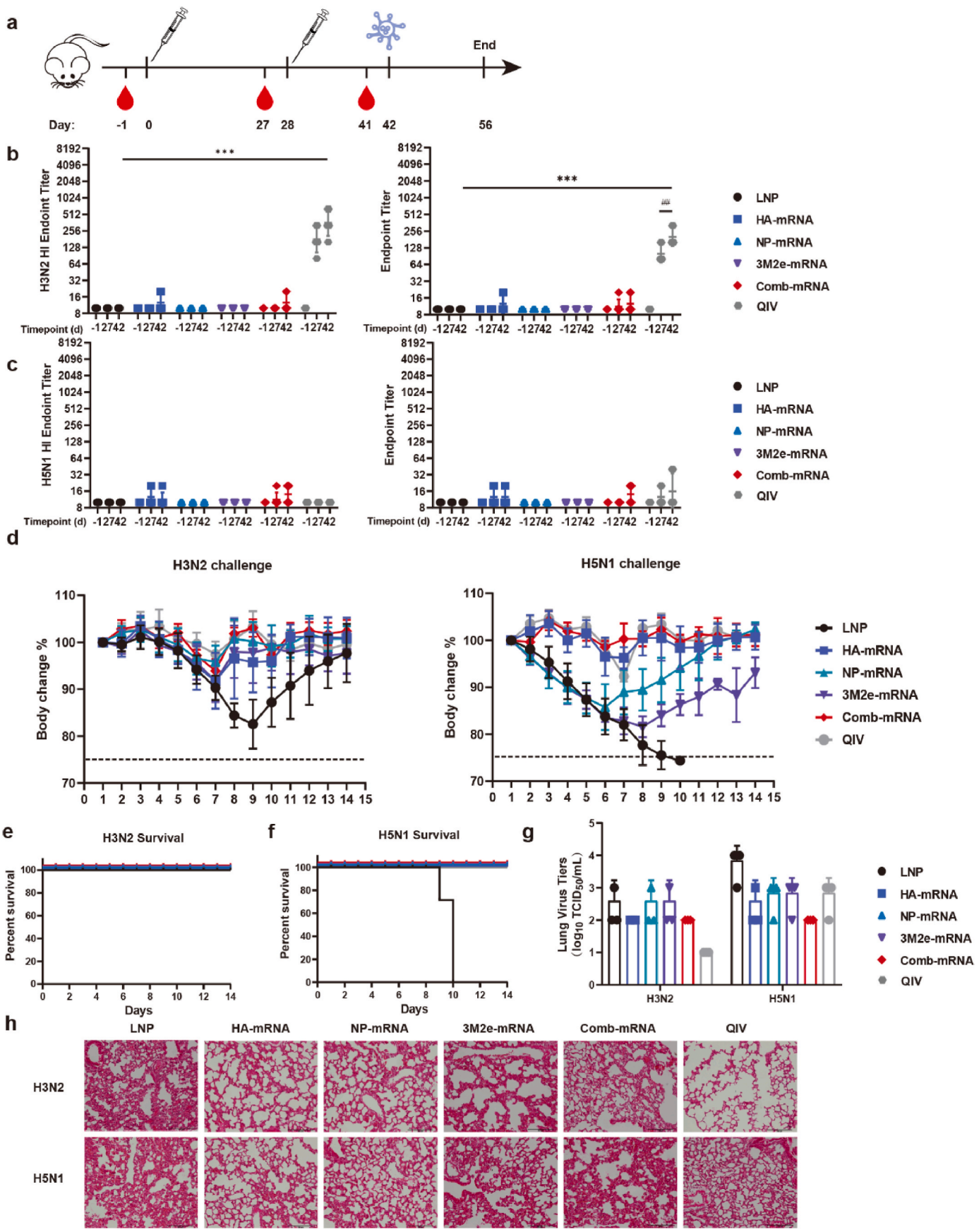


Fig. 3. Robust T cell immune response elicited by the Comb-mRNA influenza vaccine. (a) Mice were vaccinated with two doses of with the LNP, HA-mRNA, NP-mRNA, 3M2e-mRNA, Comb-mRNA and 2021–2022 quadrivalent influenza virus vaccine (QIV) (4.5 μg per mouse per dose) 28 days apart; cytokine production by $CD4^+$ and $CD8^+$ T cells in spleen cells was analyzed by flow cytometry at day 40. IFN-γ in $CD4^+$ T cells and IFN-γ and IL-2 in $CD8^+$ T cells were analyzed across four groups. Each symbol represents one animal; error bars indicate SEM. Data are from two independent experiments, analyzed by the unpaired *t*-test.



(caption on next page)

Fig. 4. Protection in mice immunized with mRNA influenza vaccine from lethal challenge by H3N2 and H5N1 viruses. (a) Mice received two doses of LNP, HA-mRNA, NP-mRNA, 3M2e-mRNA, Comb-mRNA and 2021–2022 quadrivalent influenza virus vaccine (QIV) (4.5 μg per mouse) 28 days apart. Blood samples were collected on days −1, 27, and 41 and mice were challenged with H3N2 and H5N1 influenza viruses on day 42. (b) HI and (c) micro-neutralization titers were measured for different mRNA vaccines at days −1, 27, and 41 after vaccination, with each point representing an individual animal. Lines indicate group geometric means (n = 6). Data are geometric means ± 95% CIs, analyzed by two-way ANOVA with multiple comparisons. (d) Weight changes in mice challenged with 10^5TCID$_{50}$ H3N2 and 5LD$_{50}$ H5N1 influenza viruses 14 days after booster immunization (n = 6). Kaplan–Meier survival analysis after the challenge with (e) 10^5TCID$_{50}$ H3N2 and (f) 5LD$_{50}$H5N1 viruses. (g) Viral load and (h) pulmonary lesions were assessed in mice from each group 4 days after H1N1 virus challenge (n = 3 per group).

the Comb-mRNA group. Comb-mRNA displayed significantly higher HI titers compared to initial immunization, although no notable difference was observed between initial and booster immunizations in the HA-mRNA group.

Micro-neutralization assays using strain A/Beijing/501/2009 (H1N1) were conducted to measure neutralizing antibody levels (Fig. 2c). HA-mRNA induced titers of 63.5 after initial immunization and 113.1 after booster; NP-mRNA and 3M2e-mRNA groups lacked detectable neutralizing antibodies; and Comb-mRNA showed titers of 100.8 and 201.6 for vaccinations. Booster immunization led to higher micro-neutralization titers in experimental groups, though the difference was not significant. Specific IgG levels in serum after primary and booster immunization were measured to assess the immunogenicity of HA and Comb-mRNA vaccines and their correlation with HI and micro-neutralization results (Fig. 2d).

An H1N1 influenza virus challenge in Balb/c mice was performed to evaluate the efficacy of the mRNA vaccine. Following the protocol, each mouse received 4.5 μg of mRNA vaccine intramuscularly. At 28 days after initial immunization and after a subsequent booster, mice were challenged with 5LD$_{50}$ of A/Beijing/501/2009 strain. Weight changes were monitored for 14 days (Fig. 2e). In the LNP-inoculated control group, two mice died on day 8, three on day 9, and one on day 10. No mortality occurred in the remaining groups, with significantly different survival rates from the control group (Fig. 2h). The HA-mRNA group experienced less body weight fluctuation, and the Comb-mRNA group showed minimal weight change, indicating significant effectiveness. Lung pathology and viral load assessment four days after the challenge revealed significant lesions in lungs of control mice, milder lesions in lungs of single-immunized mice, and virtually no lesions in the Comb-mRNA group (Fig. 2f and g).

A group of quadrivalent influenza-vaccinated (QIV) control mice was also included. In these mice, HI and micro-neutralizing titers were slightly higher than all of the mRNA vaccinated groups. Upon challenge, the QIV-immunized mice experienced no mortality and minor body weight fluctuations. Compared to the Comb-mRNA group, these mice exhibited less significant weight loss and fewer changes.

3.3. *Influenza mRNA vaccine stimulates cellular immune responses in mice*

To examine the cellular immune response induced by mRNA vaccines encoding HA, NP, and 3M2e antigens, we evaluated $CD4^+$ and $CD8^+$ T cell responses. We analyzed $CD4^+$ and $CD8^+$ T cell activation in mouse spleen lymphocytes 12 days after booster immunization (Fig. 3a). Previous studies have shown that nucleotide-modified mRNA vaccination induces a high frequency of antigen-specific $CD4^+$ helper T cells. Consistent with these reports, vaccinations with HA-mRNA, NP-mRNA, 3M2e-mRNA, and the combined vaccines resulted in higher proportions of IFN-γ. Notably, HA-mRNA and the triple vaccine induced a robust $CD8^+$ T cell response, with up to 10% of $CD8^+$ T cells expressing IFN-γ and IL-2. In particular, the triple vaccine elicited a more potent cellular immune response, with significant antiviral potential (Fig. 3b).

3.4. *Influenza mRNA vaccine exhibits broad-spectrum anti-influenza action*

To assess the broad-spectrum efficacy of HA-mRNA, NP-mRNA, 3M2e-mRNA, and the combined vaccine, we examined their protective potential against two influenza A subtypes, H3N2 and H5N1. Mice were vaccinated as previously described and given a booster dose 28 days later (Fig. 4a). Serum samples were collected before initial vaccination, 28 days after initial vaccination (prior to the booster), and 14 days after the booster. We evaluated the serum's inhibitory effect on the virus and the potency of neutralizing antibodies using HI and micro-neutralization assays, respectively, to determine the cross-protective efficacy of the vaccine against different viral subtypes. Strains H3N2 and H5N1 were selected for their high pathogenicity and severe societal impact. After primary immunization, only the seasonal influenza vaccine generated neutralizing antibodies against the H3N2 strain, with other groups failing to produce such antibodies (Fig. 4b). The same trend was observed with the H5N1 strain challenge (Fig. 4c).

Mice immunized with the vaccines were challenged with H3N2 and H5N1 strains, respectively, 14 days after secondary immunization. We monitored their body weight changes until day 14 after the challenge. The control group challenged with H3N2 experienced significant weight loss, and all mice challenged with H5N1 died by day 10 (Fig. 4d–f). Mice vaccinated with individual vaccines exhibited varying degrees of weight loss under H3N2 and H5N1 challenges, but no fatalities were recorded. Remarkably, the Comb-mRNA group showed relatively stable body weight under both challenges. The QIV group also performed well, with reasonable body weight changes (Fig. 4d). Lung pathology conducted four days after the viral challenge revealed more pronounced lesions in the lungs of unvaccinated mice and lesser lesions in those of influenza-vaccinated mice (Fig. 4g and h).

A preliminary safety evaluation of the vaccine was also conducted. Important organs of the mice, including the heart, liver, spleen, lung, kidney, and brain, were subjected to hematoxylin and eosin staining, revealing no apparent lesions (Supplementary Fig. 5).

4. Discussion

The emergence of coronavirus disease 2019 (COVID-19) has significantly advanced the development of mRNA vaccine technology, demonstrating its potential in combatting infectious diseases (Barbier et al., 2022). mRNA vaccines targeting a range of viruses, including COVID-19 (Mevorach et al., 2021), human metapneumovirus (Huang et al., 2021), respiratory syncytial virus (Ginsburg and Srikantiah, 2021), Zika virus (Essink et al., 2023), Ebola virus (Kozlov, 2022), human cytomegalovirus (Struble et al., 2021), herpes simplex virus (Awasthi and Friedman, 2022), human immunodeficiency virus (Morris, 2021), and rabies virus (Alberer et al., 2017) have shown promising results in preclinical research. Notably, Moderna is developing five influenza vaccines, with its seasonal influenza mRNA-1010-P101 in Phase 3 clinical trials (NCT05566639) (Hu et al., 2022), mRNA-1020 and mRNA-1030 (NCT05333289) (Lei et al., 2023) in Phase 1 clinical trials, and mRNA-1040 and mRNA-1050 in preclinical studies (moderna, 2023). Pfizer is working on two mRNA influenza vaccines; BNT161, a seasonal quadrivalent vaccine, is in Phase 3 clinical trials (NCT05540522) (Biontech, 2023), and another self-replicating mRNA vaccine is in preclinical stages. Additionally, CureVac and GlaxoSmithKline are co-developing CVSQIV, a seasonal influenza vaccine, currently in Phase I clinical recruitment (NCT05252338) (Rzymski et al., 2023).

Currently, clinical trials of mRNA vaccines are primarily focused on

seasonal influenza, not offering protection against sudden influenza pandemics. The need for broad-spectrum influenza mRNA vaccines is evident, with research predominantly directed towards this goal. A successful broad-spectrum mRNA influenza vaccine must encode a highly immunogenic antigen that is common across all influenza virus subtypes. A recent study employed mRNA to encode full-length sequences of 20 HA antigens, aiming to trigger specific immune responses to each antigen rather than cross-immune responses (Arevalo et al., 2022). This approach successfully protected mice and ferrets from lethal influenza virus challenges. Ongoing research is exploring the use of mRNAs encoding conserved influenza antigens to elicit broader cross-immune responses (Chivukula et al., 2021; Freyn et al., 2020). Our study aligns with this approach, selecting HA, along with the conserved NP and M2e proteins, as vaccine antigens. HA is a key viral protein and the primary immunogen of influenza viruses, featuring a mutation-prone head and a conserved stem. Although encoding only the conserved stem of HA has shown some protective effects (Freyn et al., 2020), our strategy of using the full-length HA sequence aims to enhance immunogenicity. NP is crucial for viral replication and is highly conserved across influenza subtypes, making it an ideal broad-spectrum antigen. M2e, the extracellular region of the influenza virus M2 protein, is a significant protective antigenic determinant and highly conserved across subtypes. Acknowledging the limited protective efficacy of a single M2 vaccination noted by Freyn et al. (2020) we used a three-tandem M2e construct to boost vaccine immunogenicity. We also immunized mice with all three mRNA vaccines to investigate whether combining multiple influenza antigens enhances their anti-influenza efficacy.

The dosage of mRNA vaccination is crucial. A vaccine encoding 20 HAs, developed by Claudia P. Arevalo et al., protected mice from lethal viral challenge with up to 50 μg per mouse, 2.5 μg of each HA, and 50 μg of the control HA-mRNA vaccine (Arevalo et al., 2022). Chivukula et al. reported that a single dose of 2 μg of Cal09 HA-mRNA vaccine resulted in a geometric mean HI titer of 160 and conferred protection against lethal challenge, functional antibodies were also detected with doses as low as 0.4 and 0.08 μg (Chivukula et al., 2021). Meagan McMahon et al. reported that mice were vaccinated with 5 μg monovalent mRNA-LNP or with 5 μg/antigen or 1.25 μg/antigen of the quadrivalent mRNA-LNP, all could induce cellular and humoral immune responses (McMahon et al., 2022). Norbert Pardi et al. reported that mice were vaccinated with 5 μg or 1 μg mRNA-LNP, they could protect mice against virus challenge (Pardi et al., 2022). In our study, we administered a single dose of 4.5 μg of mRNA vaccine or three vaccines at 1.5 μg of each antigen to the mice, followed by a booster 28 days later to enhance the immune response.

The efficacy of 4.5 μg mRNA vaccination in inducing functional and neutralizing antibodies was assessed. Both the single-dose HA-mRNA-vaccinated and the Comb-mRNA groups were observed to produce functional antibodies, effectively preventing the agglutination of erythrocytes by the influenza virus. HI titers were significantly higher in the HA-mRNA single-dose group than in the control group and were comparable to the HI titers after booster immunization when challenged with the H1N1 influenza virus. This finding suggests that the timing of booster vaccinations may require optimization, as we did not continuously monitor the persistence of neutralizing antibodies after single immunization. Adjusting the timing of immunization to correspond with a significant decline in neutralizing antibodies could lead to different outcomes.

The HI titer for the HA-mRNA vaccine was slightly higher than that for H3N2 upon challenge with the H5N1 strain, likely due to the greater amino acid sequence similarity between the HAs of H5N1 and H1N1 than that of H3N2. Sera from mice given a single dose of Comb-mRNA showed slightly higher HI titers against H1N1 challenge than HA-mRNA and were comparable to the QIV, likely because HA antigen is the main QIV component. After booster immunization, there was a notable increase in HI titers compared to single-dose vaccination. However, when challenged with H3N2, HI titers after Comb-mRNA immunization differed from the control group but were lower than those in the QIV group, possibly because QIV contains the HA antigen of H3N2, which is not contained in the Comb-mRNA group. In contrast, against H5N1 challenge, HI titers were higher in the Comb-mRNA group compared to both the single antigen-immunized group and QIV, although the difference was not significant. By comparing the amino acid sequences of the two hemagglutinin strains (A/Darwin/9/2021 (H3N2)-like virus and A/Wisconsin/67/2005), the sequence identity was 92.4%, which could explain the cross-protective effect of QIV on the A/Wisconsin/67/2005 strains.

All vaccinated groups obtained lethal protection against all three strains. Both H1N1 and H5N1 control mice succumbed following a 5LD50 strain challenge, with observable differences in lung tissue pathology and viral enrichment by day 4. H3N2, which is non-lethal to mice, resulted in weight loss but no fatalities. The Comb-mRNA group exhibited stable body weight under all three viral challenges. This finding suggests a cross-immunization protective effect, aligning with findings by Freyn et al. In our study, NP and 3M2e did not induce strong humoral immunity but offered protection against different virus subtypes, possibly through cellular immunity mechanisms.

Based on our experimental results, using mRNA technology to encode a broader spectrum or multiple antigens of influenza viruses is a feasible approach for developing a broad-spectrum influenza vaccine. The crucial challenge lies in identifying and utilizing conserved antigenic sequences of influenza viruses that are not only conserved but also capable of enhancing the immune response. In our study, we co-injected the full-length HA alongside the conserved NP and 3M2e. This approach produced specific, neutralizing antibodies under H1N1 challenge but offered less protection against different influenza subtypes. Future research will focus on exploring additional conserved influenza antigens or optimizing the dose ratio of the three vaccines to achieve more comprehensive protection. The strategy of Arevalo et al., which involves combining 20 HA antigens for injection, is also intriguing. However, the 50-μg dose used in their study is relatively high compared to other research and should be further optimized for practical application.

5. Conclusions

In summary, our research demonstrated that a universal mRNA influenza vaccine containing HA, NP, and 3M2e can effectively protect mice against various subtypes of the influenza A virus. This finding positions the proposed vaccine as a promising candidate for a universal influenza vaccine. Our findings underscore the potential of mRNA technology in addressing the challenges of influenza virus variability and pave the way for further advancements in universal vaccine development. However, in strengthening the timing of immunization, the screening and recombination of broad-spectrum influenza antigens need to be further explored.

Data availability

The data that support the findings of this study are available from the corresponding author upon reasonable request.

Ethics approval

The animal study was reviewed and approved by Animal Welfare and Ethics Committee of the Fifth Medical Center of the PLA General Hospital. Ethics approval number:2021-086-12.

CRediT authorship contribution statement

Yuying Tian: Writing – review & editing, Writing – original draft, Validation, Methodology, Data curation, Conceptualization. **Zhuoya Deng:** Validation, Methodology, Data curation. **Zhengran Chuai:** Methodology. **Cong Li:** Validation, Methodology. **Liangzheng Chang:**

Validation, Methodology, Data curation. **Fang sun:** Validation, Methodology. **Rui Cao:** Validation. **Hongyu Yu:** Validation. **Ruixue Xiao:** Validation. **Shuai Lu:** Validation. **Yan Xu:** Validation. **Penghui Yang:** Writing – review & editing, Conceptualization.

Declaration of competing interest

The authors declare that they have no known competing financial interests or personal relationships that could have appeared to influence the work reported in this paper.

Acknowledgements

This work was carried out in part with funding from the Basic Research Foundation (2023JCJQJJ0731) and Beijing Natural Science Foundation (L222075). We thank Home of Researchers for linguistic assistance during the preparation of this manuscript.

Appendix A. Supplementary data

Supplementary data to this article can be found online at https://doi.org/10.1016/j.virol.2024.110125.

References

Ainslie, K.E.C., Haber, M., Orenstein, W.A., 2019. Challenges in estimating influenza vaccine effectiveness. Expert Rev. Vaccines 18 (6), 615–628. https://doi.org/10.1080/14760584.2019.1622419.

Alberer, M., Gnad-Vogt, U., Hong, H.S., Mehr, K.T., Backert, L., Finak, G., et al., 2017. Safety and immunogenicity of a Mrna rabies vaccine in healthy adults: an open-label, non-randomised, prospective, first-in-human phase 1 clinical trial. Lancet 390 (10101), 1511–1520.

Andries, O., Mc Cafferty, S., De Smedt, S.C., Weiss, R., Sanders, N.N., Kitada, T., 2015. N (1)-Methylpseudouridine-Incorporated Mrna outperforms pseudouridine-incorporated Mrna by providing enhanced protein expression and reduced immunogenicity in mammalian cell lines and mice. J. Contr. Release 217, 337–344. https://doi.org/10.1016/j.jconrel.2015.08.051. Epub 2015/09/08.

Arevalo, C.P., Bolton, M.J., Le, Sage V., Ye, N., Furey, C., Muramatsu, H., et al., 2022. A multivalent nucleoside-modified Mrna vaccine against all known influenza virus subtypes. Science 378 (6622), 899–904. https://doi.org/10.1126/science.abm0271. Epub 2022/11/25.

Awasthi, S., Friedman, H.M., 2022. An Mrna vaccine to prevent genital herpes. Transl. Res. 242, 56–65.

Barbier, A.J., Jiang, A.Y., Zhang, P., Wooster, R., Anderson, D.G., 2022. The clinical progress of Mrna vaccines and Immunotherapies. Nat. Biotechnol. 40 (6), 840–854.

Biontech, 2023. Biotech pipeline products [updated 20230331]. Available from: https://www.biontech.com/de/de/home/pipeline-and-products/pipeline.html.

CDC. 2022-2023 U.S. Flu Season: Preliminary in-Season Burden Estimates [updated March 24, 2023]. Available from: https://www.cdc.gov/flu/about/burden/preliminary-in-season-estimates.htm?msclkid=ffacd4dbce3c11eca39a9738d63f1f64..

Cdc Seasonal Flu Vaccine Effectiveness Studies..

Center CNI, 2023. Weekly influenza surveillance report of China, week 7, No. 740 [updated 2023.03.30]. Available from: https://ivdc.chinacdc.cn/cnic/zyzx/lgzb/202302/t20230223_263876.htm.

Chivukula, S., Plitnik, T., Tibbitts, T., Karve, S., Dias, A., Zhang, D., et al., 2021. Development of multivalent Mrna vaccine candidates for seasonal or pandemic influenza. NPJ Vaccines 6 (1), 153. https://doi.org/10.1038/s41541-021-00420-6. Epub 2021/12/18.

Deng, L., Mohan, T., Chang, T.Z., Gonzalez, G.X., Wang, Y., Kwon, Y.M., et al., 2018. Double-layered protein nanoparticles induce broad protection against divergent influenza a viruses. Nat. Commun. 9 (1), 359. https://doi.org/10.1038/s41467-017-02725-4. Epub 2018/01/26.

Dolgin, E., 2021. The tangled history of Mrna vaccines. Nature 597 (7876), 318–324.

Essink, B., Chu, L., Seger, W., Barranco, E., Le Cam, N., Bennett, H., et al., 2023. The safety and immunogenicity of two Zika virus Mrna vaccine candidates in healthy flavivirus baseline seropositive and seronegative adults: the results of two randomised, placebo-controlled, dose-ranging, phase 1 clinical trials. Lancet Infect. Dis.

Freyn, A.W., Ramos da Silva, J., Rosado, V.C., Bliss, C.M., Pine, M., Mui, B.L., et al., 2020. A multi-targeting, nucleoside-modified Mrna influenza virus vaccine provides broad protection in mice. Mol. Ther. 28 (7), 1569–1584. https://doi.org/10.1016/j.ymthe.2020.04.018. Epub 2020/05/04.

Ginsburg, A.S., Srikantiah, P., 2021. Respiratory syncytial virus: promising progress against a leading cause of pneumonia. Lancet Global Health 9 (12), e1644–e1645.

Hald, Albertsen C., Kulkarni, J.A., Witzigmann, D., Lind, M., Petersson, K., Simonsen, J. B., 2022. The role of lipid components in lipid nanoparticles for vaccines and gene therapy. Adv. Drug Deliv. Rev. 188, 114416 https://doi.org/10.1016/j.addr.2022.114416. Epub 2022/07/06.

Heaton, N.S., Sachs, D., Chen, C.-J., Hai, R., Palese, P., 2013. Genome-wide mutagenesis of influenza virus reveals unique plasticity of the hemagglutinin and Ns1 proteins. Proc. Natl. Acad. Sci. U.S.A. 110 (50), 20248–20253. https://doi.org/10.1073/pnas.1320524110.

Hu, L., Lao, G., Liu, R., Feng, J., Long, F., Peng, T., 2022. The race toward a universal influenza vaccine: front runners and the future directions. Antivir. Res., 105505

Huang, J., Chopra, P., Liu, L., Nagy, T., Murray, J., Tripp, R.A., et al., 2021. Structure, immunogenicity, and conformation-dependent receptor binding of the postfusion human metapneumovirus F protein. J. Virol. 95 (18), e00593, 21.

Karikó, K., Buckstein, M., Ni, H., Weissman, D., 2005. Suppression of rna recognition by toll-like receptors: the impact of nucleoside modification and the evolutionary origin of Rna. Immunity 23 (2), 165–175. https://doi.org/10.1016/j.immuni.2005.06.008. Epub 2005/08/23.

Kim, H., Webster, R.G., Webby, R.J., 2018. Influenza virus: dealing with a drifting and shifting pathogen. Viral Immunol. 31 (2), 174–183. https://doi.org/10.1089/vim.2017.0141.

Kim, J., Eygeris, Y., Gupta, M., Sahay, G., 2021. Self-assembled Mrna vaccines. Adv. Drug Deliv. Rev. 170, 83–112.

Kozlov, M., 2022. Can Mrna vaccines transform the fight against Ebola? Nature 611 (7936), 439.

Krammer, F., 2019. The human antibody response to influenza a virus infection and vaccination. Nat. Rev. Immunol. 19 (6), 383–397. https://doi.org/10.1038/s41577-019-0143-6.

Lei, R., Garcia, A.H., Tan, T.J., Teo, Q.W., Wang, Y., Zhang, X., et al., 2023. Mutational fitness landscape of human influenza H3n2 neuraminidase. Cell Rep. 42 (1), 111951.

Leppek, K., Byeon, G.W., Kladwang, W., Wayment-Steele, H.K., Kerr, C.H., Xu, A.F., et al., 2022. Combinatorial optimization of Mrna structure, stability, and translation for Rna-based therapeutics. Nat. Commun. 13 (1), 1536. https://doi.org/10.1038/s41467-022-28776-w. Epub 2022/03/24.

Martinon, F., Krishnan, S., Lenzen, G., Magné, R., Gomard, E., Guillet, J.-G., et al., 1993. Induction of virus-specific cytotoxic T lymphocytes in vivo by liposome-entrapped Mrna. Eur. J. Immunol. 23 (7), 1719–1722. https://doi.org/10.1002/eji.1830230749.

McMahon, M., O'Dell, G., Tan, J., Sárközy, A., Vadovics, M., Carreño, J.M., et al., 2022. Assessment of a quadrivalent nucleoside-modified Mrna vaccine that protects against group 2 influenza viruses. Proc. Natl. Acad. Sci. U.S.A. 119 (45), e2206333119 https://doi.org/10.1073/pnas.2206333119. Epub 2022/11/03.

Mevorach, D., Anis, E., Cedar, N., Bromberg, M., Haas, E.J., Nadir, E., et al., 2021. Myocarditis after Bnt162b2 Mrna vaccine against covid-19 in Israel. N. Engl. J. Med. 385 (23), 2140–2149.

moderna, 2023. Moderna mrna pipeline [updated 2023.03.31]. Available from: https://www.modernatx.com/research/product-pipeline.

Morris, L., 2021. Mrna vaccines offer hope for hiv. Nat. Med. 27 (12), 2082–2084.

Ozdilek, A., Paschall, A.V., Dookwah, M., Tiemeyer, M., Avci, F.Y., 2020. Host protein glycosylation in nucleic acid vaccines as a potential hurdle in vaccine design for nonviral pathogens. Proc. Natl. Acad. Sci. U.S.A. 117 (3), 1280–1282. https://doi.org/10.1073/pnas.1916131117. Epub 2020/01/08.

Pardi, N., Carreño, J.M., O'Dell, G., Tan, J., Bajusz, C., Muramatsu, H., et al., 2022. Development of a pentavalent broadly protective nucleoside-modified Mrna vaccine against influenza B viruses. Nat. Commun. 13 (1), 4677. https://doi.org/10.1038/s41467-022-32149-8. Epub 2022/08/10.

Rzymski, P., Szuster-Ciesielska, A., Dzieciątkowski, T., Gwenzi, W., Fal, A., 2023. Mrna vaccines: the future of prevention of viral Infections? J. Med. Virol.

Struble, E.B., Murata, H., Komatsu, T., Scott, D., 2021. Immune prophylaxis and therapy for human cytomegalovirus infection. Int. J. Mol. Sci. 22 (16), 8728.

Tan, L., Zheng, T., Li, M., Zhong, X., Tang, Y., Qin, M., et al., 2020. Optimization of an Mrna vaccine assisted with cyclodextrin-polyethyleneimine conjugates. Drug delivery and translational research 10 (3), 678–689. https://doi.org/10.1007/s13346-020-00725-4. Epub 2020/02/13.

Yip, C.C., Chan, W.M., Ip, J.D., Seng, C.W., Leung, K.H., Poon, R.W., et al., 2020. Nanopore sequencing reveals novel targets for detection and surveillance of human and avian influenza a viruses. J. Clin. Microbiol. 58 (5) https://doi.org/10.1128/jcm.02127-19. Epub 2020/03/07.

Zost, S.J., Parkhouse, K., Gumina, M.E., Kim, K., Diaz Perez, S., Wilson, P.C., et al., 2017. Contemporary H3n2 influenza viruses have a glycosylation site that alters binding of antibodies elicited by egg-adapted vaccine strains. Proc. Natl. Acad. Sci. U.S.A. 114 (47), 12578–12583. https://doi.org/10.1073/pnas.1712377114.